ELSEVIER

Polymer 42 (2001) 6619–6629

polymer

www.elsevier.nl/locate/polymer

Cocontinuous polymer blends: influence of viscosity and elasticity ratios of the constituent polymers on phase inversion

S. Steinmann, W. Gronski, C. Friedrich*

Institute of Macromolecular Chemistry, Albert Ludwigs University Freiburg and Freiburg Materials Research Centre FMF, Stefan-Meier-Str. 21, D-79104 Freiburg, Germany

Received 17 July 2000; received in revised form 30 January 2001; accepted 1 February 2001

Abstract

The morphological properties of melt-mixed blends with cocontinuous phase morphology composed of poly(methyl methacrylate) and polystyrene or poly(styrene–*co*–acrylonitrile) are studied. By means of digital image analysis of two-dimensional TEM pictures the mean form factor ff_{irr} was established as a classificator. For 11 blend systems phase inversion concentrations were determined in this way.

We studied the influence of viscosity and/or elasticity ratios on the phase inversion concentration. Most theories based on viscosity ratio disagree with our experimental data. The analysis of corresponding phase inversion concentrations based on elasticity ratio determined at a constant shear stress leads to a simple and good correlation.

Keywords: Polymer blends; Cocontinuous morphology; Viscosity ratio

1. Introduction

Polymer blending is an economical and attractive route to new materials with superior properties. The morphology is a key parameter controlling their properties [1]. Different types of morphologies such as dispersed, fibrillar, lamellar or cocontinuous structures are known which can be realized by melt mixing. The cocontinuous morphology is particularly interesting because both components can fully contribute to the properties of the blend. Moreover, their network-like assembly can lead to synergistic improvement of specific mechanical properties [2,3] and conductivity [4] or permeability [5]. These cocontinuous blends are therefore called interpenetrating polymer blends (IPBs) [6]. Among the most important factors influencing the type of morphology formed during processing are volume fraction, ϕ and structural parameters of the constituent polymers (such as interfacial tension σ, viscosity η, modulus G' and the corresponding ratios) as well as processing conditions expressed by characteristic frequencies ω_{char} or shear rates $\dot{\gamma}$.

Phase inversion is defined as a process in which two phases switch their functions: the former matrix becomes the dispersed phase and the former dispersed phase becomes the matrix. Cocontinuous morphologies are formed in a certain concentration range around the phase inversion concentration [7–9] which we define as cocontinuity interval. The so called phase inversion concentration is regarded as the center of the cocontinuity interval and its correct determination is of great importance.

1.1. Quantitative morphological analysis of cocontinuity

In order to determine phase inversion concentrations of prepared blend series quantitatively it is indispensable to quantify complex blend morphologies. We are aware of two different procedures of morphological analysis. Firstly, the blend material can be extracted with solvent which is selective for one of the blend components. The dimensions of the dissolved particles are determined by SEM or by a particle counter [10]. The phase inversion concentration is determined as the concentration at which after extraction the remaining material is still self-supporting [11,12] or by the solvent dispersion test SDT [13].

Secondly, the morphology can be analyzed quantitatively by image analysis of ultrathin sections or etched surfaces. In this paper we would like to focus on the second group, i.e. on the different methods of image analysis. In literature only few techniques for systematic analysis of cocontinuous morphologies have been reported. Blacher et al. [14] and Harrats et al. [15] have established the applicability of multifractal analysis to heterophase polymer blends and

* Corresponding author. Tel.: +49-761-2034746; fax: +49-761-2034709.

E-mail address: chf@fmf.uni-freiburg.de (C. Friedrich).

0032-3861/01/$ - see front matter
PII: S0032-3861(01)00100-8

have shown that the multifractal curve can be considered as a criterion of the morphology of the network.

Another method of quantitative morphology analysis is based on the so called interfacial area per volume. It is calculated from the total perimeter of the particles divided by the total area of the particles [16]. Dedecker et al. used this parameter to characterize the development of blend morphology depending on processing time. Even though they found cocontinuous structures at moderate mixing times no significant change of the interfacial area per volume unit could be seen. A further approach was conducted by Heeschen [17]. He developed a method combining two scale invariant morphological parameters called 'cocontinuity' and 'cocontinuity balance' which he implemented for the quantitative measurement of the morphology in cocontinuous PC/SAN blends. The quantitative evaluation agreed very well with the qualitatively observed morphology. Since this method is based on sophisticated mathematical and geometrical procedures we applied an image processing technique which works with the dimensionless form factor [18,19]. This enables us to quantitatively characterize the transition from spherical morphology to cocontinuity directly by evaluating the shape of the domains.

1.2. Cocontinuity and phase inversion prediction

As already mentioned, many rheophysical material parameters of the blend's constituents influence the position of phase inversion concentration and its width. Willemse et al. showed that the width of this interval is influenced by the interfacial tension [8]. In addition He et al. [7] found a narrowing of the cocontinuity interval with increasing mixing time. In a recent publication Veenstra et al. [20] revealed a direct correlation between the capillary number and the width of the cocontinuity interval under shear flow. The factors influencing the position of the phase inversion range, will be discussed below.

Experimental investigations of two-phase polymer blends have shown that for components of equal viscosity phase inversion occurs around a volume fraction of 0.5. When the component viscosities differ significantly, the phase inversion point is shifted towards compositions richer in the high viscosity component [6,21,22].

In order to predict the phase inversion point, i.e. the phase inversion concentration ϕ_{iI}, several authors have proposed semi-empirical equations based on viscosities η_i of the components (with $i = 1, 2$). Paul and Barlow [23] and Jordhamo et al. [21] proposed the following expression for the zero shear viscosity ratio p_0 according to the observations made by Avgeropoulos et al. [24]:

$$p_0 = \frac{\eta_1}{\eta_2} = \frac{\phi_{1I}}{\phi_{2I}}, \quad \phi_{2I} = 1 - \phi_{1I}. \tag{1}$$

Miles and Zurek [6], however, assume that the condition for IPB formation should more precisely be related to the effective viscosity ratio p_{eff}:

$$p_{\text{eff}} = p(\dot{\gamma}) = \frac{\eta_1(\dot{\gamma})}{\eta_2(\dot{\gamma})} = \frac{\phi_{1I}}{\phi_{2I}} \text{ or } \phi_{2I} = \frac{1}{p_{\text{eff}} + 1}. \tag{2}$$

This equation was established on the basis of only three different blend systems and the respective phase inversion concentration was only determined qualitatively. In literature the approach has proved to be suitable for predicting the phase inversion concentration in some blend systems with a viscosity ratio near unity [22].

Metelkin and Blekht [25] based their model on the Tomotika theory of phase stability [26] and the phase inversion concentration is given as:

$$\phi_{2I} = \frac{1}{1 + p_{\text{eff}} F(p_{\text{eff}})} \tag{3}$$

with

$$F(p_{\text{eff}}) = 1 + 2.25 \log p_{\text{eff}} + 1.81(\log p_{\text{eff}})^2. \tag{4}$$

Utracki [27] proposed a model being valid for blends with viscosity ratios widely different from unity based on the Krieger and Dougherty [28] theory. The addition of polymer 1 to polymer 2 and vice versa leads to an increase in the respective blend viscosities. At the point of phase inversion these blend viscosities have to be equal. With $[\eta]$ as intrinsic viscosity and ϕ_m as the volume fraction at maximum sphere packing density, the phase inversion concentration of component 2, ϕ_{2I} is determined by:

$$\phi_{2I} = \frac{\phi_m + (1 - \phi_m) p_{\text{eff}}^{1/[\eta]\phi_m}}{p_{\text{eff}}^{1/[\eta]\phi_m} + 1}. \tag{5}$$

For polymer blends the volume fraction ϕ_m is assumed to be $\phi_m = 1 - \phi_c$, in which ϕ_c stands for the percolation concentration and amounts to 0.16 for dispersions of spheres. Utracki proposes the optimal value of the intrinsic viscosity to be 1.9 and the limiting values for polymer blends to range between 1.5 and 2.5. The experimental verification of the theory was mainly done with literature data which were generated under extremely different processing conditions and evaluated with respect to different parameters: some of the data refer to torque ratios instead of viscosity ratios, for other blend systems the viscosity ratios are determined at constant loss moduli ranging from 1 kPa to 20 MPa or constant shear rates about 100 s^{-1}.

Luciani et al. [10] refer to the relative stability of networks created by coalescence during blending, again using the viscosity ratio as the main influencing parameter:

$$\phi_{2I} = 1 - \frac{p_0^2\, \Omega^2(p_0)}{p_0^2\, \Omega^2(p_0) + \Omega^2(1/p_0)}, \tag{6}$$

with $\Omega(\chi, p_0)$ as a complex function of both the viscosity ratio p_0 and observed wavelength of the distortion λ in Tomotika's equation [26]. For viscosity ratios between 0.25 and 4 Eq. (6) predicts a nearly constant phase inversion concentration with a value around 50 vol%. Luciani et al.

verified the theory with the example of only three blend systems and the respective inverse systems. The morphological evaluation is done by means of the selective extraction of the matrix phase and determination of fiber content.

Willemse et al. [9] recently developed a semi-empirical relation based on geometrical requirements for the formation of cocontinuous structures:

$$\frac{1}{\phi_{\text{disp I}}} = 1.38 + 0.0213\left(\frac{\eta_m \dot{\gamma}}{\sigma} R_0\right)^{4.2}. \quad (7)$$

This gives the lower and upper limit, respectively, of the range of volume fractions within which a cocontinuous structure can exist, as a function of matrix viscosity η_m, interfacial tension σ, minimum radius of filaments R_0 and shear rate $\dot{\gamma}$ during blending for a capillary number value of one. This model cannot be used in a predictive manner because the filament radius has to be determined experimentally first. Willemse et al. [9] checked their theory with five different blend systems lying in a very narrow range of values of $(\eta_m \dot{\gamma}/\sigma)R_0$.

The models described up to now only account for the viscous properties of the polymers. Bourry and Favis [29], however, introduced elasticity as an important parameter for the understanding of phase inversion. They made an approach based on the elasticity ratio of blend components in which the storage modulus G_i' (with $i = 1, 2$) represents the elasticity of phase i:

$$\frac{\phi_{1I}}{\phi_{2I}} = \frac{G_2'(\omega)}{G_1'(\omega)}. \quad (8)$$

Another criterion proposed by these authors is based on the ratio of the loss moduli with $\tan \delta_i = \dfrac{G_i''}{G_i'}$

$$\frac{\phi_{1I}}{\phi_{2I}} = \frac{\tan \delta_1(\omega)}{\tan \delta_2(\omega)}. \quad (9)$$

These formulas account for the tendency of the more elastic phase to form the matrix at sufficiently high concentrations [30]. Bourry and Favis [29] achieved much better agreement with their experimental data particularly at high shear rates than with predictions based only on viscous effects. Their experimental verification was based on only one blend system.

The work which has been done up to now in the field of phase inversion in polymer blends reveals that further investigation concerning the influence of viscosity and elasticity ratio has to be done. Most studies are founded on a very small databasis with only few blend series. Since there is a need for more detailed experimental verification of the different theories we realized the evaluation of a large number of blend series prepared and analyzed under the same conditions. Consequently, parameters like the premixing procedure and grain size of the used powder, mixing time, die geometry, shear rate, quenching conditions, procedure quantitative image analysis and the like are kept constant. We chose 11 model blend systems consisting of poly(methyl methacrylate)/polystyrene (PMMA/PS) or PMMA/poly-(styrene–*co*–acrylonitrile) (PMMA/PSAN) (PSAN with 33 wt% acrylonitrile (AN)) with a broad variety of zero shear viscosity ratios p_0 (ranging from 0.004 to 7.8) and corresponding elasticity ratios ψ_0 ranging from 7.9×10^{-6} to 234 at the processing temperature. In this study we checked the effect of both viscosity and elasticity ratio on the phase inversion concentration and compared the experimental data with the predictions given by the above-described models.

Moreover, we are interested in the rheological peculiarities displayed by polymer blends near to the phase inversion concentration. The results will be published soon [31].

2. Experimental

2.1. Materials

The polymers used were anionically synthesized PMMA, anionically synthesized PS and radically synthesized PSAN. The blend system PMMA/PSAN displays a miscibility window which depends on the AN content of PSAN. In the range of 9.4–34.4 wt% AN a lower critical solution temperature (LCST) behavior in the temperature–copolymer composition range is found [32,33]. The PSAN 1 used in blend series B8, B9 and B10 contained about 33 wt% acrylonitrile and since no LCST could be detected we assume that it was not miscible with PMMA. In order to obtain a broad variety of viscosity ratios we varied the molecular weight of both blend components. The molecular weights, polydispersity and zero shear viscosities of the blend components are given in Table 1.

Eleven series of blends were prepared, each consisting of at least three blends with varying composition around the phase inversion point. Blend series B1–B4, B6, B8 and B11 were prepared in 10 wt% intervals; series B5, B9 and B10 in

Table 1
Molecular weights, polydispersities and zero shear viscosities of the polymers used

Material	M_w (g/mol)	M_n (g/mol)	PD = M_w/M_n	η_0 (Pas) at 180°C
PS 1	33,900	30,700	1.10	2.4E2
PS 2	54,000	51,400	1.05	7.5E2
PS 3	99,600	96,700	1.02	8.7E3
PS 4	1,49,300	1,48,800	1.00	1.8E4
PS 5	2,13,000	2,05,000	1.03	5.7E4
PS 6	2,55,000	2,30,000	1.11	7.4E4
PSAN 1	97,800	44,300	2.21	4.7E4
PMMA1	12,700	11,600	1.09	3.7E3
PMMA 2	31,100	24,400	1.27	1.9E4
PMMA 3	36,500	33,200	1.10	3.8E4
PMMA 4	41,000	36,900	1.11	6.2E4
PMMA 5	45,000	41,000	1.10	2.2E5
PMMA 6	53,800	43,200	1.25	1.4E5

Table 2
Blend components and processing temperatures of the prepared blend series

Blend series	Blend components		Mixing temperature (°C)
B1	PMMA 2	PS 6	200
B2	PMMA 3	PS 3	200
B3	PMMA 5	PS 3	200
B4	PMMA 1	PS 4	200
B5	PMMA 3	PS 2	200
B6	PMMA 6	PS 2	200
B7	PMMA 6	PS 1	210
B8	PMMA 4	PSAN 1	210
B9	PMMA 4	PSAN 1	190
B10	PMMA 4	PSAN 1	180
B11	PMMA 4	PS 5	200

5 wt% intervals and B7 in 2 or 3 wt% steps. Table 2 gives an overview over the respective blend components of the different blend series.

2.2. Mixing

Prior to melt mixing, all polymers were dried in vacuum at 60°C for at least 24 h and then dry-blended for 30 min by mixing the powder consisting of granules with a grain size of about 1 mm maximum in a tumble mixer. The melt blending was carried out in a Randcastle single screw extruder RCP-MT250 equipped with a capillary die. The temperatures of mixing are given in Table 2. The average shear rate in the extruder was estimated on the basis of geometrical parameters [34] to be around 12 s^{-1} and the maximum shear rate was in the range of 200 s^{-1}. For the capillary die with a length/diameter ratio (*L*/*D*) of 35 a shear rate value of about 5 s^{-1} was approximated. The residence time was constant for all blends and amounted to around 3 min. The strands coming out of the die were immediately cooled to room temperature. The blend morphology is frozen by this procedure directly after extrusion because the glass temperatures of the blend components lie approximately 80°C above quenching temperature.

2.3. Morphological investigation

The blends were prepared for transmission electron microscopy (TEM) by cutting ultrathin sections of about 60 nm (as estimated from interference colours) using a Leica Ultracut-E microtome with a diamond knife (for quantitative morphological evaluation all extruded strands were cut perpendicular to the flow direction). This was followed by a selective staining of the PS or PSAN phase with gaseous ruthenium tetraoxide (RuO_4) [35]. TEM elastic bright field images were taken on a Zeiss CEM 902, operating at 80 kV. In the images the stained PS or PSAN domains appear black and the domains consisting of PMMA are white.

The morphology of the blends was analyzed using the SIS image processing software system (Soft Imaging System GmbH). For the form factor analysis a multitude of TEM images was evaluated to determine the form factors of several hundred finite domains belonging to the dispersed phase. On the basis of this data histograms displaying the respective form factor distribution were generated. The form factors used in this article are mean values of the corresponding form factor distributions determined by the gaussian fit procedure.

2.4. Rheological testing

The rheological characterization of the neat polymers was carried out on a CVO stress controlled rheometer (Bohlin) using parallel plate geometry (plate diameter of 25 mm). In frequency sweeps isotherms were recorded and shifted with the software Lsshift to mastercurves at the respective reference temperatures. We performed the measurements at low strain amplitudes (about 1–5%) under N_2 atmosphere to avoid decomposition.

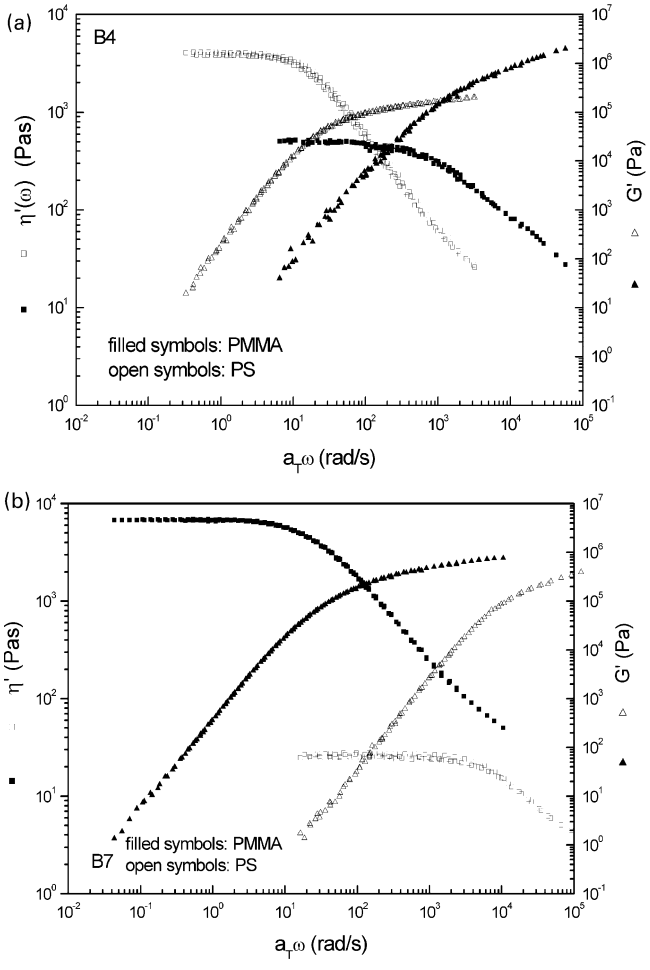

Fig. 1. (a) Storage modulus and dynamic viscosity of homopolymers of blend series B4 as functions of frequency at a reference temperature of 200°C corresponding to the processing temperature. (b) Storage modulus and dynamic viscosity of homopolymers of blend series B7 as functions of frequency at a reference temperature of 210°C corresponding to the processing temperature.

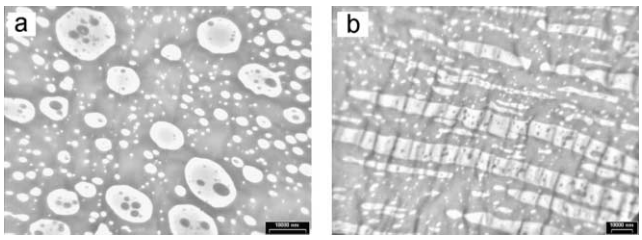

Fig. 2. TEM micrographs of a blend of series B11 with 40 wt% PMMA cut (a) perpendicular and (b) parallel to flow. PMMA is the white phase and the black phase consists of PS which is stained with RuO_4.

Two extreme examples of blends are given in Fig. 1a and b, which show the dynamic viscosities and storage moduli of the blend components at the respective processing temperature. Fig. 1a displays blend series B4 with PMMA having a much lower zero shear viscosity than the PS component which leads to a zero shear viscosity ratio of $p_0 = 7.8$. With increasing shear rates the dynamic viscosities approach and finally cross each other but the crossover lies in a shear rate range which is not reached during processing. In this study all blend series with zero shear viscosity ratios larger than 1 show a crossover of the dynamic viscosities.

Rheological properties of blend components leading to a viscosity ratio of $p_0 = 0.004$ are shown in Fig. 1b. In contrast to B4 the dynamic viscosities of the components do not cross but they also approach at higher shear rates.

3. Results and discussion

3.1. Determination of phase inversion concentration

Firstly, we want to deal with the orientation phenomena our morphologies display, which are due to the flow through the capillary die of the extruder. TEM images of the extruded strands cut perpendicular to flow direction reveal a radial orientation of the domains. With increasing distance from the center of the strands the morphology becomes finer and the orientation increases. Therefore the samples have to be morphologically investigated at the same spatial spot in order to provide comparability. In order to account for the morphology formed in the extruder we chose the center of the strands for further analysis because orientation effects are weakest there. We are aware of the fact that the morphology relaxes within the die, particularly in the middle where the shear rate becomes zero. However, the morphology develops under the given conditions in the cylinder of the extruder and does not change significantly by this relaxation.

Now we want to pass on to the comparison of blends with different morphology types investigated perpendicular and parallel to flow. For blends with low concentrations of dispersed phase the sections perpendicular and parallel to the flow direction display a different morphology. As Fig. 2a reveals, the dispersed phase consists of circular domains

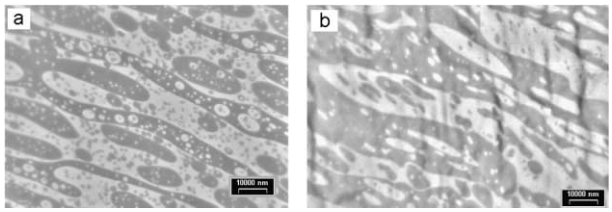

Fig. 3. TEM micrographs of a 50 wt% PMMA/PS blend of series B11 which was cut (a) perpendicular and (b) parallel to flow.

when the strands are cut perpendicular to flow. On the other hand, in the sections parallel to flow strongly elongated fibrils of the dispersed phase can be seen as shown in Fig. 2b.

Around the phase inversion concentration the blends display a different type of morphology. If the blend morphology in two sectional planes perpendicular to one another as shown in Fig. 3 is of the same type and cocontinuous in two dimensions, we assume that the blend is three-dimensionally cocontinuous.

We checked and verified this behavior with almost all blend series. Consequently, it is sufficient to analyze the morphological transition from particulate type to cocontinuous in two dimensions perpendicular to flow.

The quantitative morphological evaluation, i.e. determination of form factors, was thus performed with samples cut perpendicular to the flow direction. The form factor is a scale invariant parameter which represents the shape of finite domains in a two-dimensional image. It allows to distinguish quantitatively between spherical and cocontinuous morphologies as we will show in this section. The form factor ff is defined as follows [18,19]:

$$\mathrm{ff} = 4\pi \frac{A}{P^2}, \tag{10}$$

with A the area and P the perimeter of the domains.

Circular domains have a form factor of approximately 1, whereas the form factor of irregularly shaped domains can approach very small values.

In the following paragraphs the principles of form factor analysis will be described exemplarily with blend series B3. In Fig. 4 the morphology of three different blends of series B3 is shown. The blend with high PMMA concentration (90 wt%) displays circular PS domains (dark) dispersed in PMMA matrix (bright) according to Fig. 4a. The decrease of the PMMA concentration to 50 wt% leads to the blend morphology which is shown in Fig. 4b. The corresponding form factor histogram is presented in Fig. 5.

It can be recognized that the form factor distribution is bimodal. The form factors can thus be separated into a mean form factor $\mathrm{ff}_{\mathrm{irr}}$ of the fraction of domains which become irregularly shaped during the increase of minor phase concentration (and the respective decrease of matrix phase concentration) and another mean form factor ff_{c} which represents the fraction of domains having a circular shape. The latter also includes fibrillar domains lying perpendicular

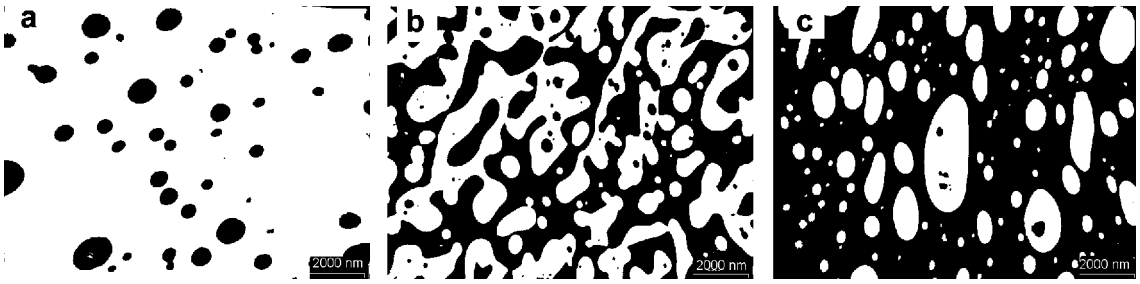

Fig. 4. Binary TEM images of PMMA/PS blends of series B3 with: (a) 90 wt% PMMA; (b) 50 wt% PMMA; and (c) 30 wt% PMMA.

to the cutting direction and not contributing to cocontinuity as discussed above. The dashed line in Fig. 5 at a form factor value of 0.8 (it was chosen empirically) represents the dividing line for the separation of the form factor distribution.

For completion in Fig. 4c one blend of series B3, with low PMMA concentration (30 wt%), with inverted phases with regard to the blend in Fig. 4a is shown.

The analysis of both mean form factors ff_{irr} and ff_c of all blends of series B3 leads to a form factor versus composition diagram as presented in Fig. 6.

Since ff_c yields values around 0.9 independent on blend composition it does not contribute to cocontinuity and is therefore neglected. The other mean form factor ff_{irr} changes with blend composition. In the range of very low and high PMMA concentrations it reaches values of about 0.7 and decreases significantly to 0.4 at 50 wt% PMMA. This minimum of ff_{irr} defines the maximum of cocontinuity and, therefore, the phase inversion concentration.

The form factor evaluation was done for all blend series. The resulting phase inversion concentrations are given in Table 3 and will be used for the verification of the theoretical predictions in the following section.

3.2. Comparison of the theoretical predictions of phase inversion concentration with experimental data

3.2.1. Viscosity ratio

For the investigation of the influence of the viscosity ratio on the phase inversion concentration not only the ratio of the zero shear viscosities p_0 but also the effective viscosity ratio p_{eff} which corresponds to processing conditions should be evaluated. Due to the validity of the Cox–Merz rule [36] for homogeneous polymer melts it is justified to use $\eta'(\omega)$ instead of $\eta(\dot{\gamma})$. The dynamic viscosities of the blend components measured at the processing temperature depending on the frequency ω can be converted into viscosities measured under steady state conditions with a shear rate $\dot{\gamma}$. The effective viscosity ratios at certain characteristic frequencies ω_{char} (see Section 2.2) were calculated by using the following equation:

$$p_{eff,\omega} = \left.\frac{\eta'_{PS\ or\ PSAN}(\omega)}{\eta'_{PMMA}(\omega)}\right|_{\omega=\omega_{char}} . \quad (11)$$

In Table 3 the corresponding blend series, the viscosity ratios, and phase inversion concentrations are listed.

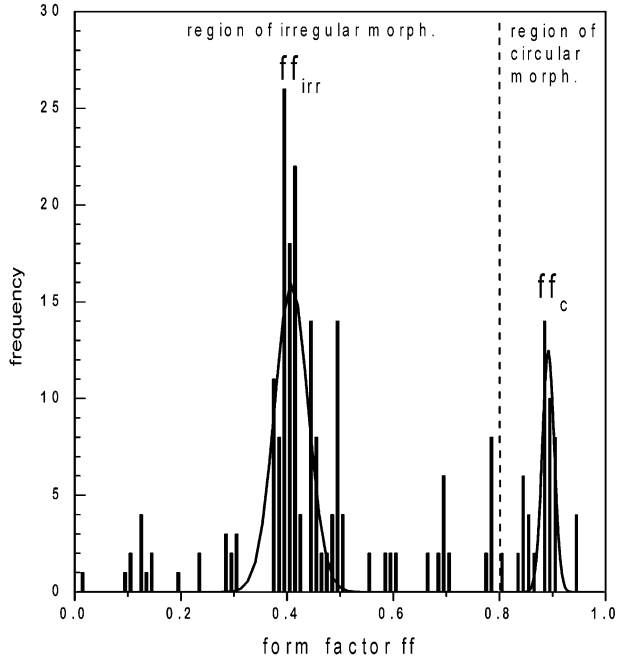

Fig. 5. Form factor distribution of a blend of series B3 with 50 wt% PMMA with cocontinuous morphology corresponding to Fig. 4b.

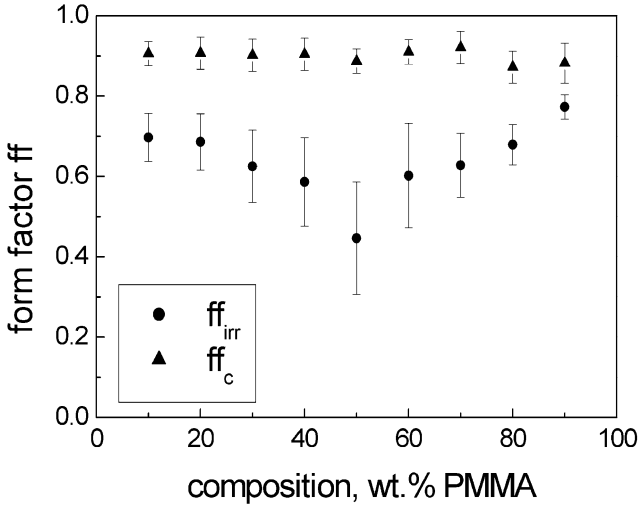

Fig. 6. Distribution of the two mean form factors ff_{irr} and ff_c depending on the blend composition for series B3.

Table 3
Zero shear viscosity ratios p_0, effective viscosity ratios under processing conditions $p_{\mathrm{eff},\omega}$ and experimental phase inversion concentrations $\phi_{\mathrm{PI,PMMA}}$ of the investigated blend series determined from form factor analysis

Blend series	$p_0 = p_{\mathrm{eff},\omega}$ at $\omega_{\mathrm{char}} \to 0$ rad/s	$p_{\mathrm{eff},\omega}$ at $\omega_{\mathrm{char}} \cong 12$ rad/s	$p_{\mathrm{eff},\omega}$ at $\omega_{\mathrm{char}} \cong 200$ rad/s	$\phi_{\mathrm{PI,PMMA}}$ (wt% PMMA)
B1	5.96	1.52	0.20	50
B2	0.24	0.27	0.28	65
B3	0.06	0.07	0.12	50
B4	7.20	5.88	0.70	55
B5	0.03	0.04	0.16	65
B6	0.01	0.02	0.15	80
B7	0.004	0.005	0.025	63
B8	1.48	0.79	0.39	45
B9	0.93	0.38	0.26	40
B10	0.77	0.29	0.22	40
B11	1.20	0.59	0.27	45

An overview over the theoretical predictions within a wide viscosity ratio range is given in Fig. 7 and the experimental data evaluated at different frequencies corresponding to Table 3 are marked. The viscosity ratios belonging to the same blend series are linked with a straight horizontal line (dotted for the PMMA/PSAN blends). For reasons of clarity error bars are left out. The errors in PI concentration are estimated to be ±5 wt% because the blends were mostly prepared in 10 wt% intervals.

Firstly, we want to focus on the viscosity ratios at zero shear conditions and the corresponding detected phase inversion concentrations of the blend series. The graph in Fig. 7 shows that the phase inversion is shifted towards concentrations equal or higher than 50 wt% PMMA for $p_{\mathrm{eff},\omega}(\omega_{\mathrm{char}} \to 0) < 1$. Exceptions are blend series B9 and B10 which undergo phase inversion at 40 wt% PMMA. In the range of $p_{\mathrm{eff},\omega}(\omega_{\mathrm{char}} \to 0) \geq 1$ the phase inversion takes place at around 50 wt% PMMA.

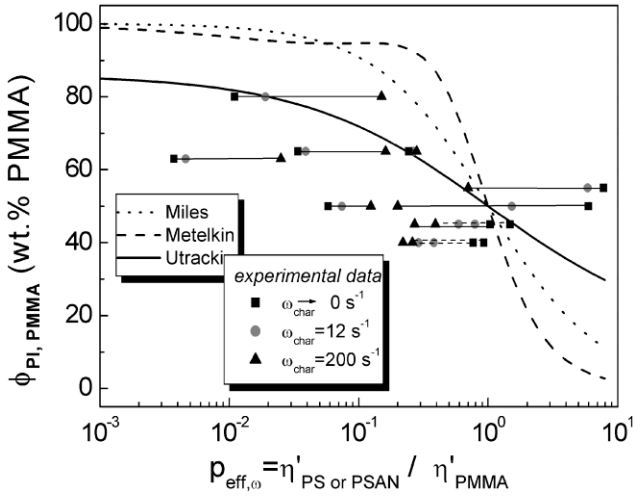

Fig. 7. Influence of the effective viscosity ratio at different characteristic frequencies on the phase inversion concentration ϕ_{PI}, which was determined by form factor analysis. The phase inversion concentration is fitted according to Eq. (2) of Miles and Zurek [6] (dotted line), Eq. (3) of Metelkin and Blekht [25] (dashed line) and Eq. (5) of Utracki (full line).

Looking at the effective viscosity ratios at mean and maximum processing shear rates it becomes clear that all blend series with PSAN as second component (B8–B10) display a ϕ_{PI} below 50 wt% PMMA. This may be caused by the fact that this system might be partially miscible and thus the domains we analyze with TEM could represent PMMA-rich and PSAN-rich mixed phases, respectively, with varying content of second component.

In the following paragraphs the experimental data will be compared to the predictions made by the models. In the viscosity ratio range of $p_{\mathrm{eff},\omega} < 1$ all models predict a shift of the phase inversion concentration to PMMA contents higher than 50 wt% in the blends. This tendency is in accordance with most of our experimental data except those of the PMMA/PSAN blends and series B11 at higher shear rates as discussed above. At viscosity ratios larger than 1, however, the two relevant blend series B1 and B4 do not undergo phase inversion at PMMA concentrations less than 50 wt% as predicted by the models. Miles and Zurek [6] and Metelkin and Blekht [25] overestimate the shifting of the PI concentration towards higher concentrations of the more viscous component substantially. For $p_{\mathrm{eff},\omega}$ values of 0.1 for example, the predictions of the phase inversion concentration amount to 91 wt% (Miles and Zurek) or 95 wt% PMMA (Metelkin and Blekht) and are still increasing with decreasing viscosity ratio. It has to be noted that both models are limited: the approach of Miles and Zurek was only confirmed for blends with nearly isoviscous components. Metelkin and Blekht did not solve the function $F(p_0)$ numerically but processed experimental data of PE/rubber blends. Thus this model can be applied to other blend systems only in a restricted way.

The model of Utracki yields the best agreement with the experimental data in comparison with the other models. For $p_{\mathrm{eff},\omega} \ll 1$ and $p_{\mathrm{eff},\omega} \ll 1$ he introduces an upper and a lower limit for the PI concentration: $\lim_{p_{\mathrm{eff},\omega} \to 0} \phi_{2\mathrm{I}} = \phi_{\mathrm{m}}$ and $\lim_{p_{\mathrm{eff},\omega} \to \infty} \phi_{2\mathrm{I}} = 1 - \phi_{\mathrm{m}}$. Utracki proposes a value of 0.84 for the maximum packing density ϕ_{m}, that means a blend component cannot form the matrix if its concentration lies below 16 vol%. This estimation is based on ϕ_{c} for

homogeneously dispersed hard spheres in a matrix. The proposed intrinsic viscosity of the dispersed phase amounts to 1.9. However, we believe that $\phi_c = 1 - \phi_m$ reaches higher values for real blend systems because the phases are deformable and a homogeneous distribution of domains is unlikely. Therefore we varied both $[\eta]$ and ϕ_m in order to fit the Utracki Eq. (5) to our experimental data at $\omega_{char} \rightarrow 0$. The resulting fit is shown in Fig. 8.

In the Utracki equation the intrinsic viscosity diverges to 2.5 with bounds set to 1.5 and 2.5 and ϕ_m reaches a value of 0.67. That means that the percolation threshold ϕ_c for our system amounts to 33 vol%.

Altogether it can be said that the Utracki model with modified parameter ranges does not overestimate the influence of viscosity ratio in contrast to the other models. The fitting procedure leads to a more flattened curve representing the weak dependence of ϕ_{PI} on $p_{eff,\omega}$ in the whole range of effective viscosity ratios. Moreover, Luciani and Jarrin [10] have made similar observations concerning a plateau-like behavior of ϕ_{PI} over a large range of viscosity ratios. The empirical relation (Eq. (17)) which is also displayed in Fig. 8 will be discussed later on.

According to Han [37] the viscosities of the blend components should be compared at a constant level of shear stress, i.e. constant G″ since the stresses are continuous across the interphase in polymer blends while the deformation rates are not. Up to G″ values of 5×10^4 Pa this evaluation in our case leads to viscosity ratios which are similar to the respective zero shear viscosity ratios. The stress predominant in our extruder is estimated to be about 10^4 Pa at shear rates of around $12\ s^{-1}$ (see Section 2.2). This is only a rough estimation which yields approximate values on which we can base our evaluation. The evaluation of viscosity ratios on the basis of constant stress with $G''_{char} = 10^4$ Pa is not performed because it yields the same results as the zero shear viscosity ratio analysis.

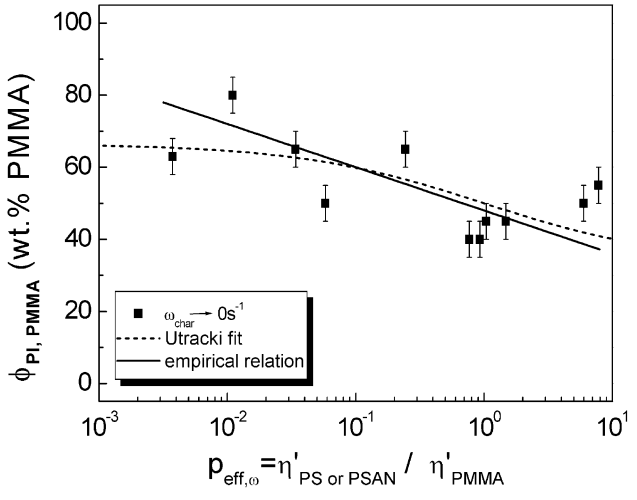

Fig. 8. Fit of the Utracki Eq. (5) to the experimental zero shear viscosity ratios depending on phase inversion concentration (dashed line) and influence of the p_0 ratios on ϕ_{PI} according to an empirical relation (17) (straight line) developed in the section of elasticity ratios.

3.2.2. Elasticity ratio

In this section the influence of elasticity ratio on PI concentration will be discussed. The elasticity ratio can be evaluated in two ways: firstly, in analogy to the evaluation of viscosity ratios the elasticities, represented by the storage moduli G', of the two blend components can be determined at the same frequency. This frequency should correspond to shear rates predominant in the melt blending equipment or to zero shear rate conditions. The obtained elasticity ratio depends on both frequency and temperature as in the case of the viscosity ratio. The second method is based on the above-mentioned proposal by Han [37] to use the appropriate criteria (here the elasticity ratios) at constant stress, which means at constant G'' [37]. It should be mentioned that the log G' versus log G'' plot is independent of the temperature, as first reported by Han and Lem in 1982 [38] on the basis of a molecular viscoelasticity theory for monodisperse [39] and polydisperse homopolymers [40]. Therefore the elasticity ratios determined by this method remain constant regardless of the mixing temperature employed as in the case of blend series B8–B10.

Both strategies were applied in the following equation and the corresponding elasticity ratios which are named $\psi_{eff,\omega}$ in the first case and $\psi_{eff,G''}$ in the latter case were calculated by using the following equations:

$$\psi_{eff,\omega} = \left.\frac{G'_{PS\ or\ PSAN}(\omega)}{G'_{PMMA}(\omega)}\right|_{\omega=\omega_{char}} \quad \text{and}$$
$$\psi_{eff,G''} = \left.\frac{G'_{PS\ or\ PSAN}(G'')}{G'_{PMMA}(G'')}\right|_{G''=G''_{char}}. \tag{12}$$

The corresponding elasticity ratios together with the characteristic frequencies and loss moduli are summarized in Table 4.

The ratios at constant shear stress G'' lie in the range of 1–10 with one exception for B7. That means PS or PSAN is more elastic than PMMA in nearly all cases. But at very high G'' values the ratio switches because PMMA has a higher plateau modulus than PS or PSAN. In contrast to the ratios at constant G'' the respective shear rate dependent ratios $\psi_{eff,\omega}$ of the blend series are spread over a wide range of values from 7.9×10^{-6} up to 234.

Fig. 9 shows the effective elasticity ratios determined at different relevant shear rates, shear stress and the corresponding phase inversion concentrations. Again the straight horizontal lines are link the different shear rate dependent ratios of the respective blend series. The distribution of the elasticity ratios with the phase inversion concentration in Fig. 9 looks quite similar to that of the viscosity ratios in Fig. 7.

The phase inversion concentration according to Bourry and Favis [29] is given by Eq. (8) which can be transformed

Table 4
Zero shear elasticity ratios ψ_0, effective elasticity ratios under processing conditions at different characteristic frequencies $\psi_{\text{eff},\omega}$ and at constant loss modulus $\psi_{\text{eff},G''}$

Blend series	$\psi_0 = \psi_{\text{eff},\omega}$ at $\omega_{\text{char}} \to 0$ rad/s	$\psi_{\text{eff},\omega}$ at $\omega_{\text{char}} \cong 12$ rad/s	$\psi_{\text{eff},\omega}$ at $\omega_{\text{char}} \cong 200$ rad/s	$\psi_{\text{eff},G''}$ at $G''_{\text{char}} = 1 \times 10^4$ Pa
B1	234	7.7	0.94	2.7
B2	0.15	0.18	0.30	2.3
B3	0.02	0.03	0.11	5.1
B4	200	115	6.44	2.5
B5	0.002	0.004	0.033	1.6
B6	1.4×10^{-4}	8.9×10^{-4}	0.023	1.2
B7	7.9×10^{-6}	3.1×10^{-5}	5.1×10^{-4}	0.6
B8	25.6	2.56	0.63	3.3
B9	16.9	0.66	0.38	3.3
B10	1.30	0.41	0.29	3.3
B11	1.83	1.30	0.45	1.9

to Eq. (13) and is presented in Fig. 9 by a dashed line.

$$\phi_{2I} = \frac{\psi_{\text{eff}}}{\psi_{\text{eff}} + 1}. \tag{13}$$

This phenomenological approach does not at all agree with the tendency displayed by the experimental data. The approach leads to the opposite behaviour.

A quite good correlation between the phase inversion concentration and elasticity ratio is achieved by a linear fit of the experimental data at constant G''_{char} value of 10^4 Pa. The linear fit on the semi-logarithmic scale is given in Eq. (14) and is marked in Fig. 9 as a straight line.

$$\phi_{\text{PI}} = -0.34 \log(\psi_{\text{eff},G''}) + 0.67. \tag{14}$$

This correlation reveals that $\psi_{\text{eff},G''}$ has a strong influence on the phase inversion concentration. Small changes of the elasticity ratio lead to strong changes of ϕ_{PI}.

In several papers the influence of the elasticity ratio on morphology development is discussed [41–44] and some formulae are generated describing its influence on ϕ_{PI} [29] as shown above. But in our case the evaluation of $\psi_{\text{eff},\omega}$ or $\psi_{\text{eff},G''}$ does not yield new knowledge: for our nearly monodisperse polymers and well defined systems we find a direct correlation between viscosity and elasticity ratios according to a power law (Eq. (15)) as shown in Fig. 10:

$$p_{\text{eff}} = \psi_{\text{eff}}^{\beta}. \tag{15}$$

For the shear rate dependent data the exponent β amounts to 0.45 and for the stress dependent data a β value of 2.7 is obtained. The resulting correlations are $p_{\text{eff},\omega} \propto \psi_{\text{eff},\omega}^{0.45}$ at constant shear rate and $p_{\text{eff},G''} \propto \psi_{\text{eff},G''}^{2.7}$ at constant G″ with $G''_{\text{char}} = 104$ Pa. That means that the

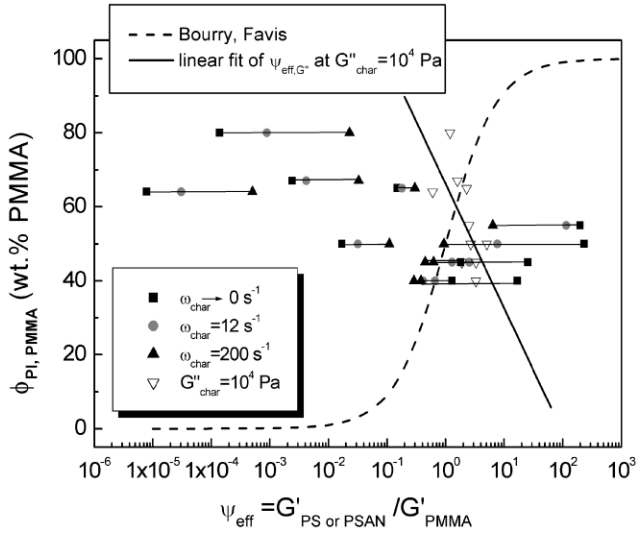

Fig. 9. Influence of the effective elasticity ratio at different characteristic frequencies ω_{char} or at a characteristic loss modulus G''_{char} on the phase inversion concentration ϕ_{PI}, which was determined by form factor analysis. The dashed line displays the approach of Bourry and Favis [29] according to Eq. (13). Moreover, the phase inversion concentration is fitted to the experimental data at a constant G''_{char} value of 10^4 Pa (Eq. (14), straight line).

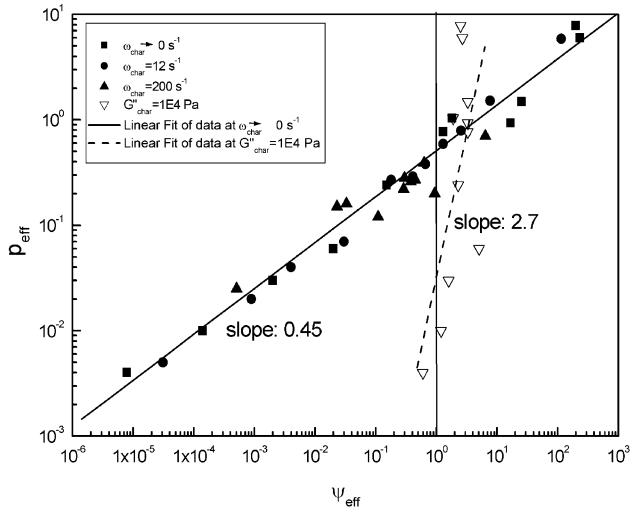

Fig. 10. Correlation between the effective elasticity ratios and the effective viscosity ratios at different frequencies or at a characteristic loss modulus. The two straight lines are linear fits of the respective data.

effects of the viscosity and elasticity ratios on phase inversion concentration cannot be separated.

Due to this direct correlation of ψ_{eff} and p_{eff} the dependence of the phase inversion concentration on the zero shear viscosity ratio can be calculated on the basis of the discussed relation between the effective viscosity ratios which says that $p_{\text{eff},G''}(G''_{\text{char}} = 10^4\ \text{Pa}) \cong p_{\text{eff},\omega}(\omega_{\text{char}} \rightarrow 0)$.

The exact power law correlation between the viscosity and elasticity ratios derived from Fig. 10 is given in Eq. (16).

$$\log(p_{\text{eff},G''}) = 2.7 \log(\psi_{\text{eff},G''}) - 1.5. \tag{16}$$

The insertion of Eq. (16) into Eq. (14) leads to the following expression:

$$\phi_{\text{PI}} = -0.12 \log(p_{\text{eff},G''}) + 0.48. \tag{17}$$

This empirical relation (17) is marked in Fig. 8 as a straight line displaying a moderate slope and fitting well to the experimental data. This again proves that the viscosity and the elasticity ratios correlate according to the above-discussed relation (16).

4. Conclusions

4.1. Quantitative morphological characterization of ϕ_{PI} on the basis of ff_{irr}

The phase inversion concentration of PMMA/PS and PMMA/PSAN blends prepared by single screw extrusion was quantitatively analyzed. By means of image analysis the transition from a spherical morphology to cocontinuity was characterized by the form factor of finite domains in two-dimensional TEM pictures. Since a bimodal form factor distribution was found for the higher concentrated blends a separation into two different mean form factor values ff_c and ff_{irr} was realized. It could be demonstrated that the minimum of the mean form factor of the irregularly shaped domains ff_{irr} represents the maximum in cocontinuity and thus yields the phase inversion concentration. For binary polymer blends with sufficient contrast in TEM imaging this method presents a fast and reliable method for the determination of phase inversion concentration.

4.2. Influence of the viscosity and elasticity ratios on the phase inversion concentration ϕ_{PI}

It is shown that most known formulae for the calculation of the phase inversion concentration depending on the viscosity ratio fail in the case of our blend systems. The Utracki equation with modified parameter ranges, especially for the ϕ_c, allows a quantitative description of experimental data.

A theoretical approach of Bourry et al. concerning the influence of the elasticity ratio on the phase inversion concentration describes a tendency which is opposite to our data. We found a good correlation of the elasticity ratios evaluated at constant shear stresses (loss modulus) with ϕ_{PI} describing a strong change of ϕ_{PI} in the case of a small change of elasticity ratio. Due to the fact that for our blend systems a strong correlation between the viscosity and elasticity ratios exists, a corresponding equation on the basis of the viscosity ratio was given which is of the same predictive quality as the modified Utracki equation.

In order to study blends with the same viscosity ratio but different elasticity ratios a selectively filled second blend component has to be used. Work in this direction is under progress.

Acknowledgements

Thanks are given to the DFG for financial support within the SFB 428. Furthermore, we want to thank BASF AG Germany for supplying the polystyrene and the poly(styrene–*co*–acrylonitrile). Thanks are also due to Röhm Germany for kindly providing the poly(methyl methacrylate).

References

[1] Paul D, Newman S. Polymer blends, vols. 1, 2. New York: Academic Press, 1978.
[2] Cook WD, Zhang T, Moad G, van Deipen G, Cser F, Fox B, O'Shea M. J Appl Polym Sci 1996;62:1699–708.
[3] Hourston DJ, Schäfer F-U. Polymer 1996;37(16):3521–30.
[4] Yang Y, Westerweele E, Zhang C, Smith P, Heeger AJ. J Appl Phys 1995;77(2):694–8.
[5] Nunes SP. TRIP 1997;5(6):187–92.
[6] Miles IS, Zurek A. Polym Engng Sci 1988;28(12):796–805.
[7] He J, Bu W, Zeng J. Polymer 1997;38(26):6347–53.
[8] Willemse RC, Posthuma de Boer A, van Dam J, Gotsis AD. Polymer 1999;40:827–34.
[9] Willemse RC, Posthuma de Boer A, van Dam J, Gotsis AD. Polymer 1999;39(24):5879–87.
[10] Luciani A, Jarrin J. Polym Engng Sci 1996;36(12):1619–26.
[11] Veenstra H, Van Dam J, Posthuma de Boer A. Polymer 1999;40:1119–30.
[12] Everaert V, Aerts L, Groeninckx G. Polymer 1999;40:6627–44.
[13] De Roover B, Devaux J, Legras R. J Polym Sci, Part A 1997;35:917–25.
[14] Blacher S, Brouers F, Fayt R, Teyssie P. J Polym Sci, Part B 1993;31:655–62.
[15] Harrats C, Blacher S, Fayt R, Jerome R, Teyssie P. J Polym Sci, Part B 1995;33:801–11.
[16] Dedecker K, Groeninckx G. Polymer 1998;39(21):4985–92.
[17] Heeschen WA. Polymer 1995;36(9):1835–41.
[18] Rosenfeld A, Kak C. Digital picture processing. San Diego: Academic Press, 1993.
[19] Weis C, Leukel J, Borkenstein K, Maier D, Gronski W, Friedrich C, Honerkamp J. Polym Bull 1998;40:235–41.
[20] Veenstra H, Norder V, van Dam J, Posthuma de Boer A. Polymer 1999;40:5223–6.
[21] Jordhamo GM, Manson JA, Sperling LJ. Polym Engng Sci 1986;26:517.
[22] Mekhilef N, Verhoogt H. Polymer 1996;37(18):4070.
[23] Paul DR, Barlow JW. J Macromol Sci Rev Macromol Chem 1980;C18:109.
[24] Avgeropoulos GN, Weissert FC, et al. Rubber Chem Technol 1976;49:93.
[25] Metelkin VI, Blekht VS. Colloid J USSR 1984;46:425.
[26] Tomotika S. Proc R Soc Lond A 1935;150:322.
[27] Utracki LA. J Rheol 1991;35:1615–37.

[28] Krieger IM, Dougherty TJ. Trans Soc Rheol 1959;3:137.
[29] Bourry D, Favis DB. J Polym Sci, Part B: Polym Phys 1998;36:1889–99.
[30] Favis D, Chalifoux JP. Polymer 1988;29:1761.
[31] Steinmann S, Gronski W, Friedrich C.Rheol Acta 2001; submitted for publication.
[32] Suess M, Kressler J, Kammer HW. Polymer 1987;28:957–60.
[33] Stein DJ, Jung RH, Illers KH, Hendus H. Angew Makromol Chem 1974;36:89–100.
[34] Carlowitz B. Kunststoff-Handbuch: Die Kunststoffe, vol. 1. Wien: Hanser Verlag München, 1990. p. 367.
[35] Trent JS, Scheinbeim JL, Couchman PR. J Polym Sci, Polym Lett Ed 1981;19:315.
[36] Cox WP, Merz EH. J Polym Sci 1958;28:619.
[37] Han CD. Multiphase flow in polymer processing. New York: Academic Press, 1981.
[38] Han CD, Lem KW. Polym Engng Rev 1982;2:135.
[39] Han CD, Jhon MS. J Appl Polym Sci 1986;32:3809.
[40] Han CD. J Appl Polym Sci 1988;32:167.
[41] Van Oene HJ. Colloid Interface Sci 1972;40:448–67.
[42] Mighri F, Ajji A, Carreau PJ. J Rheol 1997;41(5):1183–201.
[43] Fortelny I, Kovar J. Eur Polym J 1992;28(1):85–90.
[44] Levitt L, Macosko CW. Polym Engng Sci 1996;36(12):1647–55.